ISSN 1995-0780, Nanotechnologies in Russia, 2009, Vol. 4, Nos. 1–2, pp. 45–54. © Pleiades Publishing, Ltd., 2009.
Original Russian Text © V.A. Livshits, I.V. Demisheva, B.B. Meshkov, V.P. Tsybyshev, M.V. Alfimov, 2009, published in Rossiiskie nanotekhnologii, 2009, Vol. 4, Nos. 1–2.

EXPERIMENT

A Study of Adsorption and Molecular Dynamics of Spin-Labeled Molecules on the Surface of Silica Nanoparticles

V. A. Livshits, I. V. Demisheva, B. B. Meshkov, V. P. Tsybyshev, and M. V. Alfimov

Photochemistry Center, Russian Academy of Sciences, ul. Novatorov 7a, Moscow, 119421 Russia;
e-mail: livsh@photonics.ru

Received July 17, 2008

Abstract—Stable nitroxyl radicals of different structures, hydrophobicities, and electric charges were used as spin probes for studying the adsorption and molecular dynamics of the adsorbed molecules on the surface of LEVASIL silica nanoparticles. Neutral hydrophobic probes, namely, spin labeled derivatives of indole, are not adsorbed on the nanoparticles; however, the microviscosity and hydrophobicity of their environment differ from those in aqueous solutions. pH in the LEVASIL suspension is measured using a probe with an amino group. A study of the adsorption of a series of positively charged spin probes with hydrocarbon substituents of different lengths showed that the hydrophobic interactions do not contribute to their binding to the nanoparticle surface. The binding constants, the average number of negatively charged adsorption centers per nanoparticle, and the surface potential were determined from the adsorption isotherms of the radical cations. The rotational mobility parameters of the adsorbed radicals were estimated after analysis of the EPR line shape. A dependence of these parameters on the total spin probe concentration is observed. This is explained by the rapid dynamic equilibrium (chemical exchange) between the adsorbed and unbound spin probes. The chemical exchange rates are estimated. A slow increase in adsorption in the equilibrium nanoparticle suspension (with a characteristic time of ~10^4 min) and a change in adsorption isotherms (accompanied by a change in the dynamical parameters of the adsorbed particles) are detected. Slow changes in these parameters are attributed to the existence of sufficiently deep energy traps (pores) where the adsorbed radicals slowly diffuse. The rotational mobility of the radicals in these pores is less than in the surface adsorption centers.

DOI: 10.1134/S1995078009010054

INTRODUCTION

In recent years, functional nanoparticles based on silica have received much attention. They are used as nanosized fluorescence materials, quantum dots, chemosensors, and biosensors [1–9]. The advantage of silica nanoparticles as a basis for these devices is their higher stability compared to organic polymer matrices and the possibility of modifying the surface and protecting the interior (for hollow nanoparticles) from environmental exposure, particularly to oxygen.

LEVASIL silica sols from H.C. Starck GmbH & Co. KG. (Germany) are among the most promising representatives of this class of materials. LEVASIL sols are aqueous colloidal dispersions of amorphous silica particles with excellent stability and resistance to gelling. LEVASIL sols are produced from molecularly dissolved silicic acid by means of a growth process. The particles are stabilized in part by small quantities of alkali (pH 8–11). This results in a negative charge on the silica particles.

To build functional nanomaterials based on silica sols and to control the properties of these materials, one has to study the microstructure of the nanoparticles and the dynamics of molecules added to sols. We used the spin probe method to do that in this work. In recent decades it has been clearly demonstrated that spin probes and labels give important and sometimes unique information on the structure, dynamics, and intermolecular interactions in various microheterogeneous physicochemical and biological systems [10–15].

EXPERIMENTAL

Some physicochemical parameters of LEVASIL 200/30 sols are given in Table 1 [16]. One can see from the table that the average particle diameter is 15 nm, which corresponds to the specific surface area of 200 m^2 per 1 g. The solids content in the suspension is 30%.

Table 1. LEVASIL 200/30 silica sols

Solids concentration	30%
Na_2O titratable content	0.15%
Density	1.2 g/cm^3
Viscosity	max. 5 mPa s
Specific surface area	200 m^2/g
Average particle size	15 nm
pH value	9
Storage stability	18 months

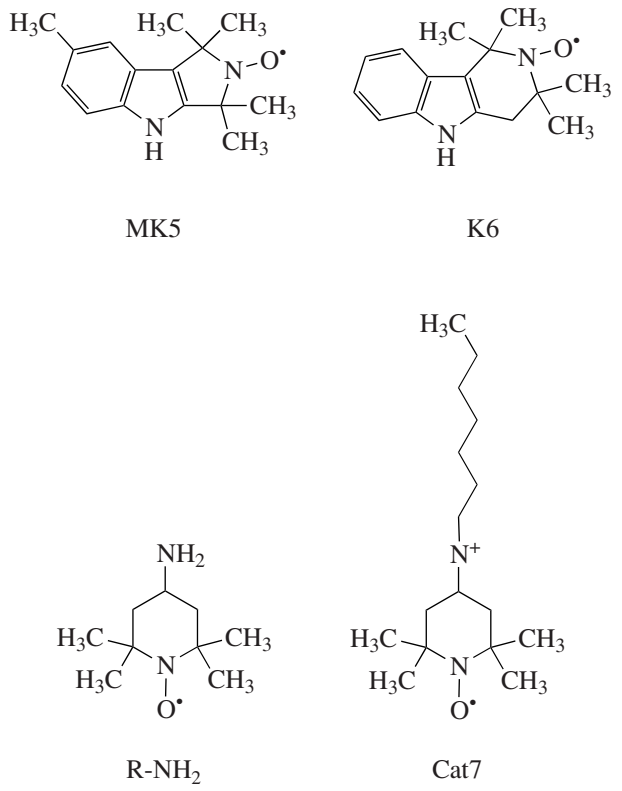

Fig. 1. Structures of spin probes.

We used nitroxyl radicals of different structures, hydrophobicities, and charges as spin probes and studied their EPR spectra vs. nanoparticle and probe concentration, ionic strength, and time. We used spin probes that could be sensitive to various microregions of LEVASIL sol suspension: hydrophobic spin probes MK5 and K6, RNH_2 radical, and a series of positively charged spin probes Cat7–Cat12 with hydrocarbon substituents of different lengths. The structures of these radicals are shown in Fig. 1. MK5 and K6 radicals were kindly provided by Dr. A.B. Shapiro (Institute of Chemical Physics, Russian Academy of Sciences), the RNH_2 radical was from Aldrich (Germany), and Cat7–Cat12 radicals were kindly provided by Prof. G.B. Khomutov (Department of Physics, Moscow State University).

Spin probes MK5 and K6 are only weakly soluble in water and exhibit an affinity to hydrophobic regions [11]. They are chemical isomers in which the reporter NO group is located in a rigid five-membered planar pyrrolidine ring (MK5) or in a nonplanar conformationally labile piperidine ring (K6). RNH_2 radical has a NH_2 group whose charge depends on pH of the environment. Since the charge changes can cause redistribution of the electron and spin density, this radical can serve as a pH-sensitive spin probe.

Cat7–Cat12 radicals bear positive charge on the quaternary nitrogen atom, which is almost constant at pH 3–10. Hence, these probes should be sensitive to the charge and potential of the nanoparticle surface. In addition, the presence of *n*-alkyl groups of different lengths in these radicals may make it possible to assess the contribution of hydrophobic interactions to their binding with the surface of silica nanoparticles.

EPR spectra of the spin probes were recorded using a Bruker ER 200D spectrometer at a constant temperature to within ±0.5°C. EPR spectra were recorded at low microwave power (18 dB, $H_1 \approx 0.0625$ G) and low modulation amplitude to exclude distortions of the EPR line shape.

The concentrations of free spin probes and their complexes in solution were determined by double integration of the EPR spectra and by comparison with standard solutions of a nitroxyl radical 4-hydroxy-2,2,6,6-tetramethylpiperidin-1-oxyl (TEMPOL).

EPR spectra of the spin probes were numerically simulated using a model of nonspherical (anisotropic) rotation, in which a spin probe was characterized by the coefficients of rotational diffusion with respect to the symmetry axis ($R_\parallel$) and the perpendicular axes ($R_\perp$) and the angle β between the *z*-axis of magnetic tensors (*A*, *g*) and the symmetry axis of the diffusion tensor. Calculations were performed using software [17], in which these parameters, as well as individual line widths, were determined using nonlinear least-squares fitting and a modification of the Levenberg–Marquardt minimization algorithm.

Additionally, in order to characterize the rotational dynamics of the spin probes, the effective rotational correlation times of spin probes were determined from the EPR spectra by assuming isotropic rotation and using the following relationship [18]:

$$\tau_{\text{eff}} = 6.65 \times 10^{-10} \Delta H_{+1} ((I_{+1}/I_{-1})^{1/2} - 1), \qquad (1)$$

where $I_{\pm 1}$ are the amplitudes of the hyperfine structure (HFS) components ($m = \pm 1$) and ΔH_{+1} is the width (defined as the distance between the extrema) of a low-field HFS component.

The polarity of the environment of a spin probe was characterized by constant *a* of the isotropic HFS on the N^{14} nucleus and by dimensionless hydrophobicity parameter *h*, defined as the following [19]:

$$h = \frac{a_W - a}{a_W - a_{HC}}, \qquad (2)$$

where a_{HC} and a_W are the values of *a* in toluene and in water, respectively. $h = 1$ under hydrophobic conditions (in toluene), and, in water, $h = 0$.

RESULTS

The interaction of the spin probes of each group with LEVASIL 200/30 nanoparticle suspension is considered below.

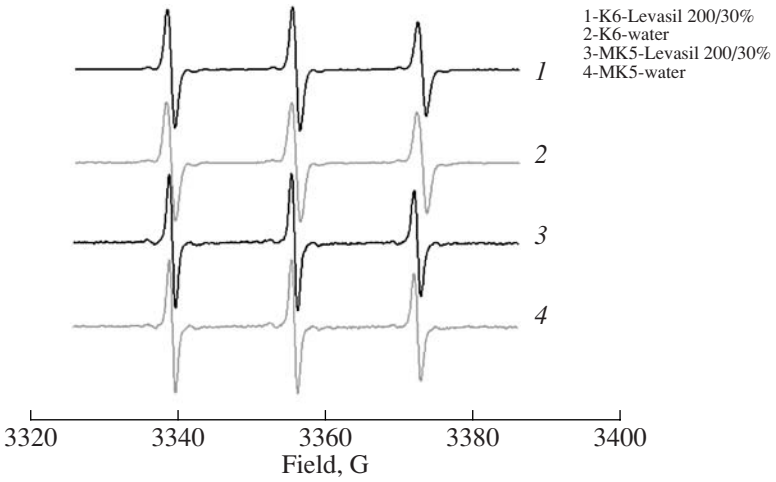

Fig. 2. EPR spectra of K6 and MK5 radicals (*1*, *3*) in LEVASIL 200/30 suspension and (*2*, *4*) in water at 293 K.

1. Hydrophobic Probes MK5 and K6

EPR spectra of K6 radical in water and LEVASIL 200/30 suspension (Fig. 2) are very similar and correspond to the rapid, almost isotropic, rotation of radicals. Similarly, EPR spectra of MK5 probe in water and in the nanoparticle suspension are almost the same. This means that hydrophobic probes MK5 and K6 are not adsorbed on the nanoparticle surface. However, the quantitative analysis of EPR spectra shows that some changes occur in the nanoparticle suspension when compared to the aqueous solution. First, rotational correlation time τ_R increases from 0.066 ns in water to 0.085 ns in suspension. Second, rotation anisotropy slightly changes, which can be seen from the ratio of HFI component intensities I_0/I_{+1}: In water this ratio is less than unity, whereas in suspension it is almost unity. Third, the polarity of the spin probe environment slightly decreases in suspension: $h \cong 0.1$ vs. $h = 0$ in water. The first two factors are obviously caused by the macroscopic viscosity. The increase in h indicates that the spin probes not bound to the nanoparticles, nevertheless, are sensitive to their microenvironment, probably because of the changes in the structure of water near the particle surface.

2. pH-Sensitive Spin Probe RNH_2

EPR spectra of RNH_2 radical in water and in LEVASIL 200/30 sol suspension are shown in Fig. 3.

The quantitative analysis of these spectra allows the following conclusions. (1) The rotational correlation time of the radical increases from 0.06 ns in water to 0.14 ns in suspension. (2) a_{iso} in suspension increases by 0.16 G as opposed to the aqueous solution (pH 7.4). (3) An additional EPR signal corresponding to the slower rotation of RNH_2 radical appears in suspension.

These differences between the aqueous solution and suspension are due to the following mechanisms. The increase in the rotational correlation time of the radical not bound to the nanoparticles, as in the case of K6, results in part from the small increase in the suspension macroviscosity. However, the relative increase in τ_R for RNH_2 is much more than for K6. This difference obviously results from the fact that some RNH_2 radicals are protonated (RNH_3^+); hence, they can bind to the negatively charged nanoparticle surface due to their positive charge and dissociate into the aqueous phase again. Upon binding, the rotational mobility of the radical drastically decreases and the effective rotational correlation time of the radical in the aqueous phase increases as a result of the rapid exchange between the bound and unbound states. Obviously, the presence of strongly immobilized EPR signals resulting from the adsorbed radicals supports this mechanism. One can see from Fig. 3 that the fraction of the adsorbed radicals is rather small; it is no more than 5%, as estimated from the simulated EPR spectra.

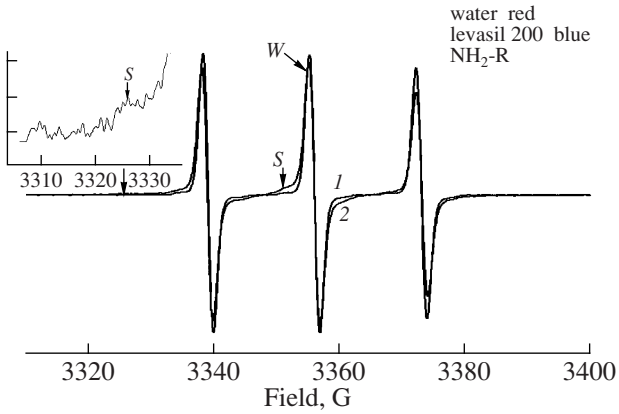

Fig. 3. EPR spectra of RNH_2 radical (*1*) in water and (*2*) in LEVASIL 200/30 sol suspension.

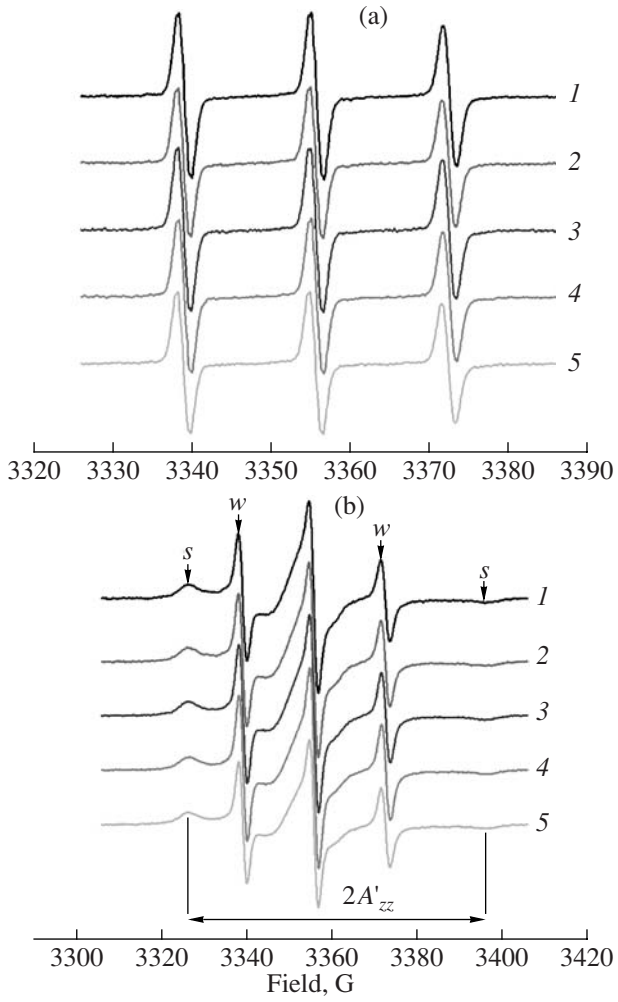

Fig. 4. (a) Spectra of Cat8–Cat12 radicals in water: (*1*) Cat8, (*2*) Cat9, (*3*) Cat10, (*4*) Cat11, and (*5*) Cat12. Spin probe concentration is 10^{-4} M. (b) Spectra of Cat8–Cat12 radicals in LEVASIL 200/30 suspension: (*1*) Cat8, (*2*) Cat9, (*3*) Cat10, (*4*) Cat11, and (*5*) Cat12. Spin probe concentration in suspension is 10^{-3} M.

The increase in a_{iso} is also caused by the pH dependence of the charge and, therefore, the electron and spin density distribution of RNH_2 radical. Similar pH dependences are known for a series of nitroxyl radicals that have an ionizable NH_2 group (e.g., see [20]). pK values for primary amino groups of aliphatic amines are about nine; therefore, in LEVASIL suspension, where pH ≅ 9 [1], approximately half of the RNH_2 radicals are uncharged, and the other half are protonated (positively charged). The observed signal of fast rotation from the "free" radicals results from the overlap of these two signals. At the same time, most radicals are protonated and positively charged at pH 7 in water. The presence of the deprotonated RNH_2 form in the suspension results in an increase in a_{iso} of the observed total signal. To determine pH in suspension, we constructed a calibration plot of a_{iso} of the RNH_2 radical vs. pH in standard aqueous buffer solutions at pH 7–10.5. pH in LEVASIL suspension that was determined using this plot is 9.6 ± 0.1. The sample-averaged pH measured using a pH electrode is 9.9 ± 0.05. The difference between these values is somewhat larger than the experimental errors of these methods. It might be supposed that these differences result from the fact that the protonated RNH_3^+ radical is, for the most part, located near the negatively charged nanoparticle surface, where pH differs from the sample-average value.

3. Cat7–Cat12 Radical Cations

The adsorption of the radicals on the nanoparticle surface and its effect on the shape of the EPR spectra is studied more comprehensively for Cat7–Cat12 radicals, which have a positive charge (+1) in a wide pH range.

The EPR spectra of Cat8, Cat10, and Cat12 radicals in water are shown in Fig. 4a. The correlation times of these radicals only slightly increase in the Cat7–Cat12 series, from 0.090 ns to 0.096 ns (Table 2). Obviously, this weak dependence results from the segmental mobility of the hydrocarbon chain, which has a coil conformation in an aqueous solution.

Figure 4b shows the spectra of Cat8–Cat12 radicals in LEVASIL 200/30 suspension. One can see that two EPR signals are clearly seen for all three radicals in suspension, one corresponding to the fast rotation of the radical (*w*) and the other corresponding to its strong immobilization (*s*), which is obviously a result of adsorption on the nanoparticles.

The structure–dynamical parameters of Cat7–Cat12 radicals in LEVASIL suspensions are given in Table 2. For fast rotation signals corresponding to spin probes unbound to the surface, the correlation time estimated, assuming isotropic rotation, is ≅0.34 ns for Cat7 and is independent on the hydrocarbon chain length within the error of the experiment.

One can also see from Table 2 that, for all the radicals τ_R, values in suspension (with total radical concentration being 10^{-3} M) are more than twice as high as τ_R values in water. These estimates are obtained using formula (1) without taking into account partial overlap of the fast rotation signal with the strongly immobilized component. To estimate the effect of this overlap on τ_R, we simulated two-component EPR spectra where the EPR spectra of the radicals in water were taken as weakly immobilized component. Determining τ_R using formula (1) from these two-component spectra resulted in no more than a 6% difference with the signal in water. Therefore, the correlation times of the radicals unbound to the surface measured in the EPR spectra of suspensions are really much higher than for the radicals in the aqueous solution. The nature of these differences is discussed in Section 4.2.

Table 2. Structure–dynamical parameters of spin probes in LEVASIL suspension. τ_{aq} and τ_w are rotational correlation times of the spin probes not bound with nanoparticles in water and in LEVASIL suspension, respectively; A_{zz} and A'_{zz} are z-components of the HFI tensor unaveraged and partially averaged over molecular rotation; $\Delta\theta$ is the average angular libration amplitude of z-axis of the spin probe coinciding with the direction of π orbit of the unpaired electron; $D_{\|}$ is the coefficient of uniaxial rotational diffusion about the axis coinciding with the direction of the NO bond of the radical fragment of the probe; and s/w is the amplitude ratio of strongly and weakly immobilized EPR signals responsible for the spin probes bound with nanoparticles and unbound ones

Cat-n	$\tau_{aq} \times 10^{10}$ s	$\tau_w \times 10^{10}$ s	$2A'_{zz}$ (G)	$2A_{zz}$ (G)	$\Delta\theta$ (deg)	$D_{\|} \times 10^{-7}$ s^{-1}	s/w
7	0.90 ± 0.08	3.45 ± 0.25					0.1 ± 0.006
8	0.91 ± 0.08	3.5 ± 0.25	70.2 ± 0.15	75.55 ± 0.15	16.6 ± 1	1.8 ± 0.1	0.11 ± 0.01
9	0.93 ± 0.08	3.25 ± 0.25		0.2			0.1 ± 0.008
10	0.94 ± 0.08	3.15 ± 0.25		0.2			0.1 ± 0.009
11	0.95 ± 0.08	3.15 ± 0.25					0.1 ± 0.01
12	0.96 ± 0.08	3.1 ± 0.2					0.1 ± 0.007

Note that the polarity of the Cat7 environment in sol solution, as in the case of K6 probe, is somewhat lower than in water.

Because the central components of the EPR signals of the unbound and adsorbed radicals strongly overlap (Fig. 4b), the rotational mobility of the probes adsorbed on the surface was estimated using the distance between the outer extrema of the spectrum $2A'_{zz}$ (Fig. 4b), which equals twice the z-component of the HFI tensor partially averaged due to molecular rotation. The rotational mobility of the adsorbed radicals is governed by their orientation on the surface, which is unknown. It might be supposed that the rotation of Cat7–Cat12 probes consists of fast librations within a limited solid angle that result in the partial averaging of the components of the HFI tensor. In this model, the libration amplitude ($\Delta\theta$) can be estimated using the following formula [21]:

$$A'_{zz} = A_{zz}\langle \cos^2(\Delta\theta)\rangle + A_{\perp}\langle \sin^2(\Delta\theta)\rangle, \qquad (3)$$

where A_{zz} is the unaveraged (limiting) value and A'_{zz} is the value averaged over the motion of the z-component of the hyperfine interaction tensor (A).

On the other hand, if the radical is adsorbed in such a way that its long axis coinciding with the average direction of the hydrocarbon chain is on average perpendicular to the surface or, vice versa, parallel to it, a uniaxial rotation by the angle of 2π is possible around the axis, approximately coinciding with the direction of NO bond. In this case, the frequency of uniaxial molecular rotation can be estimated from A_{zz} and A'_{zz} values.

A_{zz} values were determined at 77 K for the samples in which the weakly immobilized component of the unbound spin probes was almost absent at 293 K. To make these samples, we concentrated LEVASIL suspension by a rotor evaporator until the volume decreased to approximately two thirds of the initial and used low radical concentrations to ensure their complete binding to the surface.

The measured A_{zz} values are given in Table 2. The components $A_{\perp}$ were taken as equal 6 G. The libration amplitudes found according to formula (3) are approximately 14 degrees at 293 K (Table 2). To determine the rotational diffusion coefficient, we simulated the EPR spectra of the measured A_{zz} within the uniaxial diffusion rotation model using the software package of Freed et al. [17]. The calibration plots of A'_{zz} vs. $D_{\|}$ were constructed from the calculated EPR spectra. The coefficients of uniaxial rotation around the axis, coinciding with the x-axis (the direction of NO bond) of the radical, were determined from the calibration plots. These values are also given in Table 2.

The choice between these models of motion can be based on the fact that $\Delta\theta$ or $D_{\|}$ are independent of the alkyl residue length (Section 4.1). The lack of this dependence shows that hydrocarbon chains do not contribute to binding. This means that the radical orientation where the hydrocarbon groups have no contact with the nanoparticle surface is more probable as a binding model.

The adsorption of Cat type radicals was studied more comprehensively as a function of alkyl residue length, radical concentration in solution, and ionic strength.

4.1. Effect of the Alkyl Residue Length

Figure 4b shows the EPR spectra of Cat8, Cat10, and Cat12 radicals in LEVASIL 200/30 suspension. In all spectra, the weakly immobilized component (w) corresponds to the radical in solution, whereas strongly immobilized component (s) corresponds to the adsorbed radicals. First, the changes show that the shape of both components is almost the same for all the radicals of this series. Second, the amplitude ratio of the strongly and weakly immobilized components (s/w) which quantitatively characterizes the adsorption is also almost the same (Table 2).

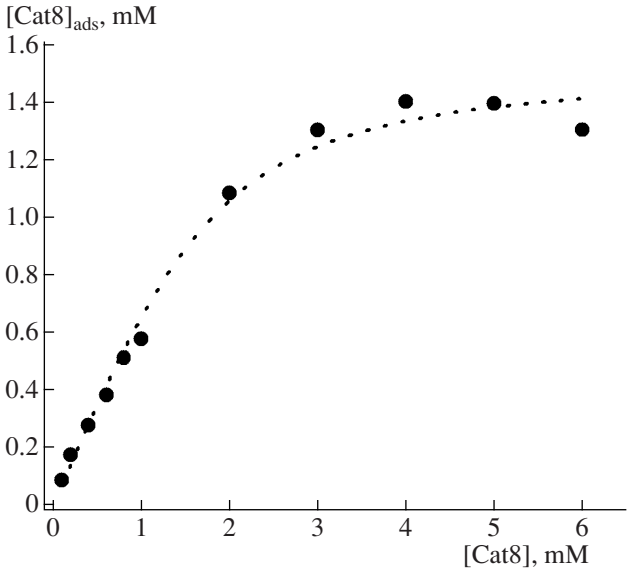

Fig. 5. Experimental concentration of adsorbed radicals derived from the amplitude of immobilized EPR signals of Cat8 radical in LEVASIL 200 7.5% suspensions (dots) and best fit within the model of radical binding with adsorption centers (formula (3)) constructed by nonlinear least squares (dashed line).

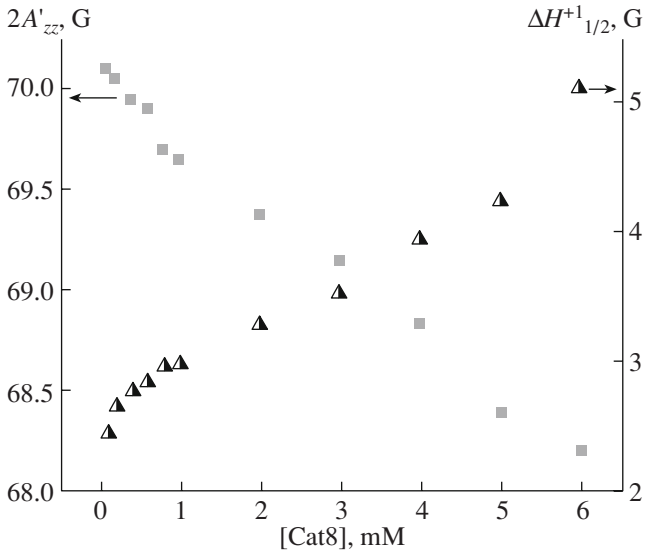

Fig. 6. The distance between the outer extrema of the immobilized EPR signal (parameter $2A'_{zz}$) and half-width at half-height of the low-field component of the immobilized EPR signal ($\Delta H^{+1}_{1/2}$) as a function of the total Cat8 concentration in LEVASIL 7.5% suspension.

These results demonstrate that the adsorption of Cat radicals does not depend on the length of the alkyl group in the radical, which brings us to the conclusion that the contribution of hydrophobic interactions to the adsorption is rather small or lacking. This conclusion is supported by the study of the effect of ionic strength on adsorption (see below). Therefore, further experiments were performed mainly with Cat8.

4.2. Effect of Spin Probe Concentration in Suspension

First, we studied the amplitudes of strongly and weakly immobilized EPR signals as functions of the radical concentration in the initial 30% suspension. It was found that the amplitude of the strongly immobilized component (corresponding to the adsorbed radicals) increases nearly linearly, while the amplitude of the weakly immobilized component (corresponding to the unbound radicals) linearly decreases. The exception is the high concentration region (5–10 mM), where the EPR line shape of the unbound spin probes may be affected by the spin exchange between these probes. These relationships result from the large number of binding sites on the surface proportional to the total area of the nanoparticle surface. Therefore, the initial suspension concentration was reduced to 7.5%.

Next, the intensities of the low-field component ($m = +1$) of the strongly immobilized EPR signals in the 7.5% suspension were expressed directly through the bulk concentrations in mM. To do this, we first simulated two-component EPR spectra at the lowest total Cat8 concentration in the undiluted 30% suspension (10^{-4} M). In these conditions the amplitude ratio of the weakly and strongly immobilized signals is minimal. The line shapes of the strongly and weakly immobilized components were simulated within the model of convolution of gaussian and lorentzian line shapes. Next, relative fractions of weakly and strongly immobilized components were varied until the best fit to the experimental spectrum was found. It was found that the fraction of *w*-component is about 9%. Therefore, the amplitude of the strongly immobilized component of this spectrum corresponds to 0.91×10^{-4} M. This relationship was used then to convert the amplitudes of the low-field components into the bulk concentrations. The resulting curve is shown in Fig. 5.

To determine the adsorption parameters, namely, the binding constant and the number of adsorption centers, we simulated this dependence using simple "chemical" binding model.

$$K_a = \frac{c_b}{(c_0^{sl} - c_b)(c_{ads} - c_b)}, \qquad (4)$$

where K_a, c_0^{sl}, c_b, and c_{ads} are the binding constant with the adsorption center, the initial concentration of the spin probes, the concentration of the bound probes, and the concentration of the adsorption centers, respectively. All the values are expressed through bulk molar concentrations. The simulation was performed by nonlinear least squares using the equation based on formula (4). The simulation (fitting) results are also given in Fig. 5.

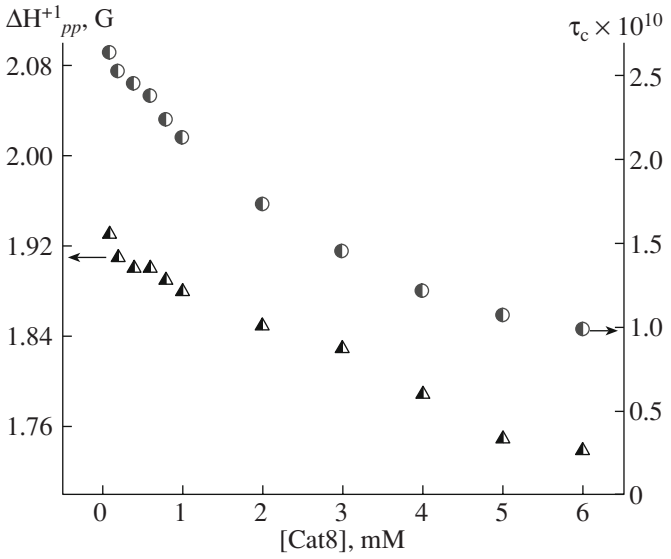

Fig. 7. Width between maximum inclination points of the $m = +1$ component of EPR signal (ΔH_{pp}^{+1}) and rotational correlation time of spin probes Cat8 not bound with the surface (τ_R) as a function of the total Cat8 concentration in LEVASIL 200/7.5 suspension.

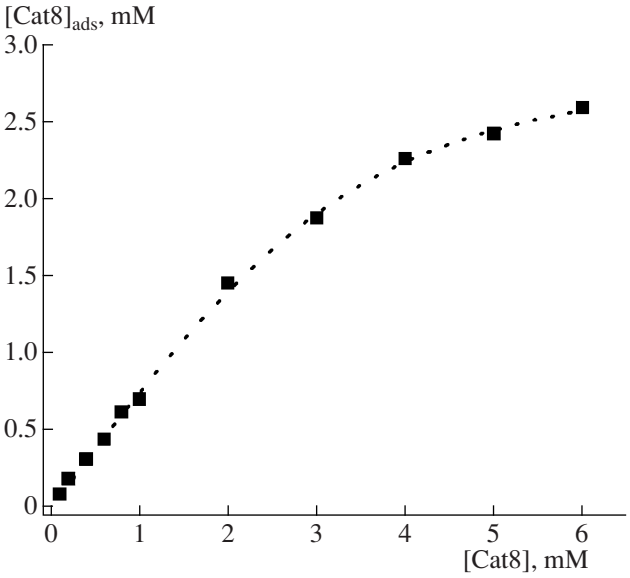

Fig. 8. Experimental concentration of adsorbed radicals as a function of their total concentration, taking into account the changes in the EPR spectra shape due to the chemical exchange between adsorbed and free radicals (dots) and the best calculated isotherm obtained by nonlinear least squares (dashed line).

From the adsorption curve fitting, the binding constant $K_a = 2.7 \times 10^3$ M^{-1}. One can see from Fig. 5 that the agreement between the experimental and simulated binding isotherm is rather poor for high radical concentrations. Moreover, the amount of adsorbed radicals decreases in this range as the concentration increases, which obviously disagrees with the simple adsorption mechanism.

To find the origin of this abnormality of the adsorption isotherm, we measured the parameters of the adsorption-induced (immobilized) EPR signal as functions of the total Cat8 radical concentration. The parameters $2A'_{zz}$ and half-width of the low-field component of this signal are shown in Fig. 6.

One can see from Fig. 6 that the parameters $2A'_{zz}$ and $\Delta H_{1/2}^{+1}$, characterizing the molecular mobility of the adsorbed radical, depend substantially on the total radical concentration in the system. Namely, the rotational mobility of the adsorbed radicals increases with the radical concentration. This manifests itself as a decrease in $2A'_{zz}$, i.e., the increase in the averaging of anisotropy of hyperfine interaction, and as an increase in $\Delta H_{1/2}^{+1}$, i.e., the increase in the relaxation line broadening. This unusual behavior in adsorption can be the result of two things. The first is the structure–dynamical heterogeneity of the adsorption centers. At low radical concentrations, the radicals are adsorbed on the centers that correspond to the low molecular mobility of the spin probes and the relatively high binding constant. As the total radical concentration increases, adsorption takes place on the centers with a higher mobility of the adsorbed molecules and, therefore, a low binding constant. However, this mechanism can hardly explain why the rather strong concentration dependence of $2A_{zz}$ and $\Delta H_{1/2}^{+1}$ remains in the range where the amount of adsorbed radicals changes only slightly. According to the other mechanism, a rapid dynamical equilibrium (chemical exchange) exists between the adsorbed radicals and the radicals in the solution, which results in a partial averaging of the anisotropic hyperfine interaction ($2A'_{zz}$) and relaxation broadening of the EPR spectra of the immobilized component.

The parameter governing the effect of chemical exchange on the immobilized component equals the product of the exchange rate constant (k_{ex}) and the fraction of the "free" probes in the solution:

$$k_b = k_{ex}(1 - P), \quad (5)$$

where P is the fraction of the immobilized radicals in the total amount of radicals. Therefore, the effect of exchange on the parameters of the EPR signal of unbound probes is governed by the product

$$k_f = k_{ex}P. \quad (6)$$

Therefore, the effect of exchange on the relaxation parameters of the immobilized signal increases and its effect on the relaxation parameters of the unbound radical decreases as the total radical concentration increases. One can see from Figs. 6 and 7 (see below) that these are the effects we observe in the experiments.

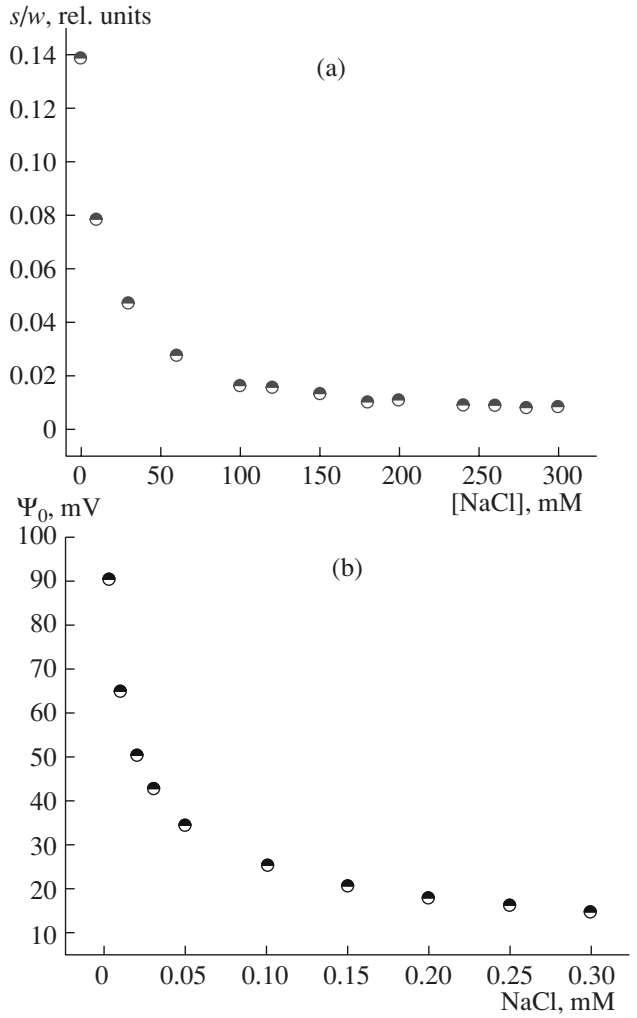

Fig. 9. (a) The ratio of the immobilized signal to the free one as a function of the NaCl concentration for Cat8. The radical concentration is 4×10^{-4} M. (b) Calculated surface potential of the nanoparticle as a function of the concentration of an inert 1 : 1 electrolyte (NaCl).

The changes in the parameters of the EPR spectra of the unbound radicals are shown in Fig. 7.

One can see from this figure that both the width of the hyperfine component and the rotational correlation time of the probe unbound to the surface decrease as the total radical concentration increases and they tend to the values typical for the free probe in water. The results obtained agree with the exchange mechanism and cannot be explained within the heterogeneity model.

The broadening of the immobilized component due to the chemical exchange decreases its amplitude. Therefore, we chose the product of the amplitude and the line half-width as a parameter characterizing the change in the fraction of the immobilized component as a function of the total radical concentration. This parameter, which characterizes the integral intensity similarly to the intensity of $m = +1$ component (Fig. 5), can be converted to the concentration scale. As a result, we obtain the adsorption isotherm that takes into account the change in the shape of the EPR signal of adsorbed radicals due to the chemical exchange (Fig. 8).

One can see from Fig. 8 that taking into account the change in the shape of the immobilized EPR signal as the total radical concentration increases eliminates the "unphysical" decrease in the concentration of adsorbed radicals (Fig. 5) and substantially improves the agreement between the experimental and simulated isotherms.

From the fitting of the improved adsorption curve, the binding constant is 1.97×10^3 mol^{-1}. The amount of adsorption centers per particle of the LEVASIL 200/30 sol was also estimated using the bulk concentration of these centers obtained from fitting. This value averages 87 centers, and the surface concentration of the adsorption centers is about 12 centers per 100 nm^2 of the surface.

With the obtained isotherm and numerical values of the relaxation broadening due to chemical exchange (Fig. 8), one can estimate the rate of chemical exchange (dissociation–association) of the radicals with the binding centers. Thus, for total radical concentration of 1 mM, we obtain from Fig. 8 that $P = 0.76$ and additional relaxation broadening from Fig. 6 is ≈0.5 G. Using formula (3) we obtain $k_{ex} \approx 3.5 \times 10^7$ s^{-1}. This high rate of chemical exchange indicates relatively weak binding of the radicals with the adsorption centers.

4.3. Effect of Ionic Strength

The adsorption was studied as a function of the ionic strength of the suspension in order to assess the contribution of electrostatic interactions to the adsorption of Cat radicals.

It is known from the works performed earlier by H.C. Starck GmbH that an increase in the ionic strength up to 0.3 M has little effect on the stability of sol suspensions; specifically, it has no effect on the sol–gel transition. Hence, the concentration range of the neutral electrolyte NaCl used for varying the ionic strength was 0–0.3 M.

Figure 9a shows the amplitude ratio of the EPR signals from the adsorption centers and unbound radicals as a function of NaCl concentration. One can see from formula (2) that the ratio of the immobilized signal to the free one characterizes the binding constant for low concentrations, where the concentration of adsorbed radicals linearly depends on the total radical concentration in suspension, because the factor $c_{ads} - c_b$ in the denominator is approximately constant at $c_{ads} \gg c_b$. One can see from Fig. 9a that, at as small an increase in the ionic strength as 0.3 M, this ratio decreases by a factor of 13 almost to zero. The obtained result shows that the main contribution to binding is from the electrostatic attraction of positively charged spin probes to the negatively charged adsorption centers.

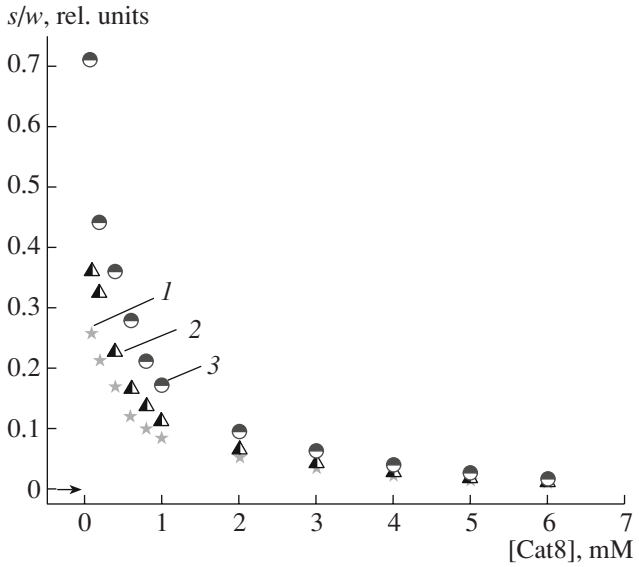

Fig. 10. The ratio of the amplitude of the low-field component ($m = +1$) of the immobilized signal to the amplitude of the component ($m = +1$) of the EPR signal of unbound Cat8 radicals as a function of the radical concentration (*1*) 30 min after sample preparation, (*2*) after 3×10^4 min, and (*3*) after ~8×10^4 min.

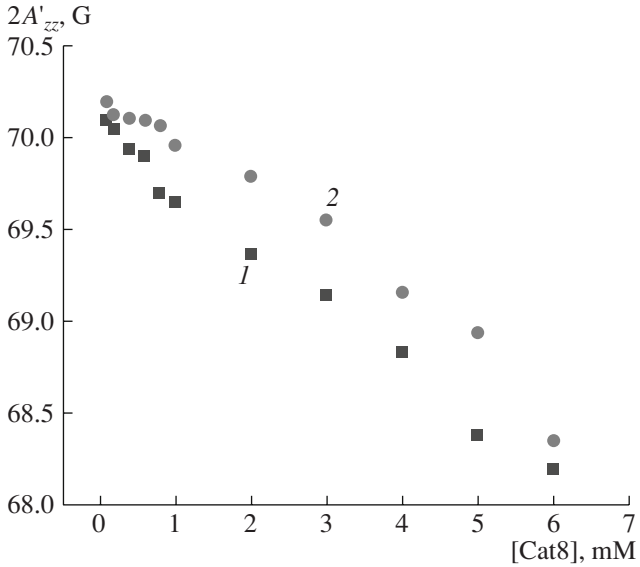

Fig. 11. Changes in the $2A'_{zz}$ parameter of the EPR spectra of adsorbed radicals at different times after sample preparation as a function of Cat8 radical concentration in LEVASIL 200/30 suspension. Squares correspond to 30 min after sample preparation; circles correspond to after ~8×10^4 min).

The surface potential as a function of the ionic strength can be estimated from the relationship following from the electrical double layer theory [21]:

$$\sigma^2 = 2000\varepsilon_0\varepsilon RT\Sigma c_i\left[e^{-z_i F\psi_0/RT} - 1\right], \qquad (7)$$

where σ is the surface charge density, $\sigma = ec_s$ (c_s is the surface concentration of negatively charged adsorption centers, c_i is the concentration of ions with the charge z_i, F is the Faraday constant, ε_0 is the electric constant, ε is the dielectric constant of water, and ψ_0 is the surface potential.

We found the surface potential of the nanoparticle as a function of the electrolyte concentration (NaCl) by numerically solving the Eq. (7). It is given in Fig. 9b. Without NaCl, the concentration of the radical itself, 4×10^{-4} M, was taken as the electrolyte concentration. One can see from Fig. 9b that the dependence of ψ_0 on the electrolyte concentration is qualitatively similar to the dependence of the experimental parameter *s*/*w*. According to the Boltzmann formula, ψ_0 governs the radical concentration in the diffuse part of the electrical double layer around the nanoparticle.

Note, however, that this estimate is rather approximate. To calculate the surface potential more exactly, one has to take into account the discrete structure of the charge distribution on the nanoparticle surface.

Slow Kinetics of Adsorption Changes

We observed that the ratio of the amplitude of the strongly immobilized signal to the EPR signal amplitude of the unbound probes slowly changes with time, and the character of these changes depends on the total radical concentration in suspension.

Figure 10 shows the ratio of the amplitude of the adsorbed radicals to the EPR signal amplitude of the unbound radicals recorded at different times after sample preparation. One can clearly see from Fig. 10 that the fraction of the adsorbed signal increases with time, and this process is more pronounced at low total radical concentrations. Measurements show that *s*/*w* increases nearly linearly with time.

We have also measured the spectral parameters of the immobilized signals, namely, $2A'_{zz}$, which characterizes the dynamics of the adsorbed probes, as a function of aging time and total radical concentration. These curves are given in Fig. 11.

One can see from Fig. 11 that $2A'_{zz}$ increases with sample aging time, that is, the mobility of the adsorbed radical (rotational mobility or chemical exchange rate) decreases. These results, together with the data on the increase in the fraction of the adsorbed radicals given in Fig. 10, can be explained by the fact that the adsorbed radicals diffuse with time into deeper traps exhibiting higher binding constants and lower mobility. The available surface binding centers are occupied by other radicals from the solution. The reason the concentrations of the adsorbed radicals change with time is probably the slow structural rearrangements in the nanoparticles themselves. The linear dependence of *s*/*w* parameters on the aging time mentioned above shows that these

structural rearrangements, or the radical diffusion processes caused by them, are far from saturation at $\approx 8 \times 10^4$ min and should be taken into account in the design of devices, particularly chemosensors based on silica nanoparticles.

CONCLUSIONS

1. Samples of silica nanoparticle suspensions that contain spin labeled molecules (spin probes) of different structures are produced. The adsorption and molecular dynamics of these molecules on the nanoparticle surface and in bulk suspensions is studied by electron paramagnetic resonance.

2. It is shown that uncharged hydrophobic spin probes, spin-labeled derivatives of indole fluorophore, are not adsorbed on the surface of LEVASIL nanoparticles; however, their rotational mobility (that is, the microviscosity of the environment) and environment polarity differ from the aqueous environment.

3. With the use of an amino derivative of a nitroxyl radical, local pH in silica nanoparticle suspensions is measured near pK of the amino group.

4. The study of adsorption of a series of positively charged spin probes with hydrocarbon substituents of different lengths demonstrated that hydrophobic interactions do not substantially contribute to the binding of these molecules.

5. The study of adsorption isotherms of radical cations made it possible to determine their binding constant with the nanoparticle surface and the amount of negatively charged adsorption centers on the silica nanoparticles.

6. The rotational mobility parameters of the adsorbed spin-labeled molecules are estimated using the EPR spectra.

7. The dependence of the dynamical parameters of the adsorbed spin probes on the total concentration of spin probes added to the suspension is found. This dependence is attributed to the existence of rapid dynamical equilibrium (chemical exchange) between the adsorbed and unbound radicals; the rate constants of chemical exchange are evaluated.

8. A slow ($\approx 10^4$ min) increase in adsorption in the equilibrium suspension of silica nanoparticles and changes in the adsorption isotherm are observed. These changes are followed by changes in the dynamical parameters of the adsorbed particles. The results obtained are attributed to the existence of relatively deep energy traps (pores) where adsorbed radicals slowly diffuse. The rotational mobility of the radicals in these traps is lower than in the surface adsorption centers. These slow changes in spatial distribution and parameters of the adsorbed molecules should be taken into account in the design of chemosensors and other devices based on silica nanoparticles. The results obtained are of interest in the development of methods for testing nanoparticle structure, dynamics of the introduced functional molecules, and the time behavior of the structure parameters of the nanoparticles.

REFERENCES

1. R. J. Reifeld, J. Noncryst. Solids **121**, 254 (1990).
2. C. J. Brinker and G. W. Scherer, *Sol–Gel Science: The Physics and Chemistry of Sol–Gel Processing* (Academic, New York, 1990).
3. W. Jin and J. D. Brennan, Anal. Chim. Acta **461**, 1 (2002).
4. A. C. Pierre, Biocatal. Biotransform. **22**, 145 (2004).
5. G. Hungerford, A. Rei, M. Ferreira, K. Suhling, and C. Tregidgo, J. Phys. Chem. **111**, 3558 (2007).
6. A. Burns, P. Sengupta, T. Zedayko, B. Barid, and U. Wiesner, Small **2**, 723 (2006).
7. A. van Blaaderen and A. Vrij, J. Colloid Interface Sci. **156**, 1 (1993).
8. W. Stoeber, A. Fink, and E. Bohn, J. Colloid Interface Sci. **26**, 62 (1968).
9. A. Burns, H. Ow, and U. Wiesner, Chem. Soc. Rev. **35**, 1028 (2006).
10. *Spin Labeling: Theory and Applications,* Ed. by L. Berliner (Academic, New York, 1976; Mir, Moscow, 1979), Vol. 1.
11. *Biological Magnetic Resonance,* Vol. 8: *Spin Labeling: Theory and Applications*, Ed. by L. Berliner and J. Reuben (Plenum, New York, 1989), Part 1.
12. *Biological Magnetic Resonance*, Vol. 22: *Very High Frequency ESR/EPR*, Ed. by O. Grinberg and L. Berliner (Kluwer Academic, New York, 2004).
13. V. A. Livshits, B. G. Dzikovskii, V. G. Avakyan, V. Yu. Rudyak, and M. V. Alfimov, Izv. Akad. Nauk, Ser. Khim., No. 5, 1139 (2005).
14. V. A. Livshits and B. G. Dzikovskii, E. A. Samardak, and M. V. Alfimov, Izv. Akad. Nauk, Ser. Khim., No. 2, 233 (2006).
15. V. A. Livshits, I. V. Demisheva, B. G. Dzikovskii, V. G. Avakyan, and M. V. Alfimov, Izv. Akad. Nauk, Ser. Khim., No. 12, 2081 (2006).
16. *Levasil: The Versatile Silica Sols with a Broad Application Spectrum* (H. C. Starck SilicaSol, Leverkusen, Germany).
17. D. E. Budil, S. Lee, S. Saxena, and J. Freed, J. Magn. Reson., Ser. A **120**, 155 (1996).
18. A. M. Vasserman and A. L. Kovarskii, *Spin Labels and Probes in Physical Chemistry of Polymers* (Nauka, Moscow, 1986) [in Russian].
19. A. N. Kuznetsov and V. A. Livshits, Zh. Fiz. Khim. **48**, 2295 (1974).
20. A. N. Tikhonov, R. V. Agafonov, I. A. Grigoriev, I. A. Kirilyuk, V. V. Ptushenko, and B. V. Trubitsin, Biochim. Biophys. Acta **1777**, 285 (2008).
21. O. Griffith and P. Jost, in *Spin Labeling: Theory and Applications*, Ed. by L. Berliner (Academic, New York, 1976; Mir, Moscow, 1979), Vol. 1.
22. R. Aveyard and D. A. Haydon, *An Introduction to the Principles of Surface Chemistry* (Cambridge University Press, Cambridge, 1973).